

Content from this work may be used under the terms of the CC BY 3.0 licence (© 2019). Any distribution of this work must maintain attribution to the author(s), title of the work, publisher, and DOI

# EXPERIMENTAL STUDIES OF RESONANCE STRUCTURE DYNAMICS WITH SPACE CHARGE\*

L. Dovlatyan<sup>†</sup>, T.M. Antonsen Jr., B.L. Beaudoin, S. Bernal, I. Haber, D. Sutter, G.D. Wyche  
 University of Maryland, College Park, MD, USA

## Abstract

Space charge is one of the fundamental limitations for next generation high intensity circular accelerators. It can lead to halo growth as well as beam loss, and affect resonance structure in ways not completely understood. We employ the University of Maryland Electron Ring (UMER), a circular 10 keV storage machine, to experimentally study the structure of betatron resonances for beams of varying degrees of space charge intensity. A grid based tune scan experimental technique is employed and results are compared to computer simulations using the WARP code.

## INTRODUCTION

In conventional circular accelerators the design goal of a focusing magnet system is to have a restoring force that varies linearly with the distance from the system center. In actuality several resonances will be driven by imperfections in the machine. The resonances excite other degrees of freedom of the beam motion which can cause instabilities, amplitude growth, and ultimately particle loss. Many of these resonances limit the beam intensity and luminosity that can be physically achieved.

As new machines aim to go to ever higher space charge intensity [1], it is clear that impacts of coulomb interactions on resonance structure dynamics must be better understood. Work has been done in generating theories and simulations of potential behavior, but not much in the way of experimental verification on an accelerator [2–5].

An ongoing experimental program at the University of Maryland Electron Ring (UMER) is focused on studying resonance behavior over a broad range of space charge intensities. UMER has the unique ability to inject a beam with a range of intensities varying from an emittance dominated 150 μA beam up to a space charge dominated 80 mA beam with a typical tune depression of 0.2. Using a set of numerical and hardware tools, we scan and map a large range of tune space revealing nonlinear resonance structure with different beam intensities.

## EXPERIMENTAL SETUP AND TOOLS

Assuming a simple hard edge model of a FODO lattice, a set of equations can be derived through matrix multiplication that relate the change in phase advance to the focusing and defocusing strengths of the quadrupoles [6]. Expanding these equations to second order gives an approximate form relating the tunes to quadrupole strengths:

$$(Q_x, Q_y) = C_0 \pm C_x k_x \mp C_y k_y + k_x k_y C_{xy} = f(k_x, k_y) \quad (1)$$

where the constants  $C_x, C_y, C_{xy}$  are functions of the effective length of quadrupoles,  $k_x$  is the strength of focusing quadrupoles (QF), and  $k_y$  is the strength of defocusing quadrupoles (QD). By varying the magnet strengths by  $\Delta k$ , tune space can be measured and mapped over a range of values. See visual representation in Figure 1.

$$(Q_x, Q_y)_{ij} = f(k_x + i\Delta k, k_y + j\Delta k) \quad (2)$$

$$i, j = 1, 2, \dots, M, \quad 1, 2, \dots, N$$

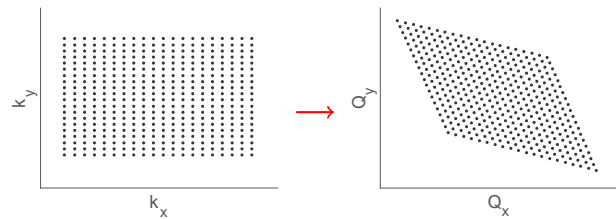


Figure 1: Visual example of mapping from quadrupole strengths to tune space using Eq. (1).

UMER’s lattice consists of a FODO design (see Figure 2) which allows the ability to experimentally run a quadrupole scan, where each focusing and defocusing quad is independently controllable. Although measurements can take a long time to complete, the gridded scans can be done in parts over different runs.

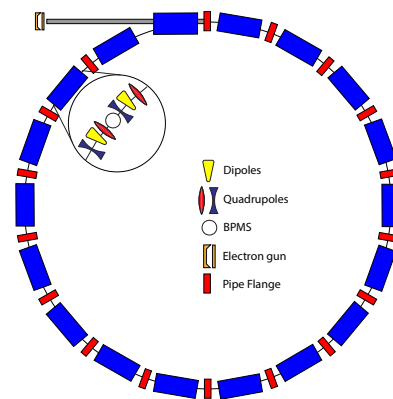


Figure 2: UMER lattice consists of 36 FODO cells around the 11.52 m circumference ring. Each cell contains two quadrupoles and one bending dipole.

\* Funding for this project provided by DOE-HEP

<sup>†</sup> Levondov@umd.edu

Tune measurements are done using all 14 available BPMs on UMER. We employ the now common NAFF algorithm to calculate fractional tunes [7]. The RF system is turned off for the measurements allowing only a coasting beam in the ring; this reduces the total number of turns available for analysis. The larger current beams survive for around ~30 turns which means NAFF measurements are done with 32 turns. To partially compensate for the low number of turns and noise, repeat tune measurements are done with multiple BPMs to have better statistical results.

## RESULTS

An initial small range scan is done with a low current (0.6 mA), low space charge, beam near the nominal operating point. 64 turns of BPM data is used to measure tunes.

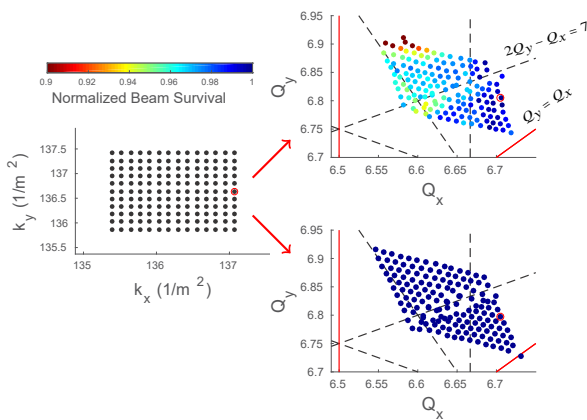


Figure 3: (top right) Experimental grid scan. (bottom right) Simulated grid scan. On the tune diagram, red lines are 2nd order and black lines are 3rd order resonances. The red circle indicates nominal operating point.

The experimental scan in Figure 3 reveals a nearby third order resonance ( $2Q_y - Q_x = 7$ ) impacting the beam. The resonance does not cause measurable current loss, but does clearly cause a split in the tune measurement across the resonance. The presence of third order resonances in UMER is interesting due to the fact that the ring has no sextupole magnets. An hypothesis is that the presence of these resonances comes from measured high order field terms in the dipole and quadrupole magnets. After adding these terms into the ring model, the simulations were able to reproduce the same resonances that appear in the experiment.

The scan also shows the start of the vertical integer stopband ( $Q_y = 7$ ) beginning around  $Q_y = 6.9$  as particles start to get lost. This gives a measure of the stopband widths of the resonances. A grid scan can be done across integer stopbands to give an experimental measure of the resonance widths. Simulations predict the integer stopbands, but have not given good agreement on the stopband widths. These stopband widths are also predicted to increase with space charge [5].

For the simulated grid scan, 10k particles were tracked using the WARP PIC code [8]. Initial conditions for the sim-

ulated beam were based on experimental measurements, i.e. emittance in horizontal and vertical planes. A semi-gaussian initial beam distribution was used. Simulations were made sure to converge with growing number of particles and decreasing cell sizes. The simulations agree closely with the experiment in regards to predicted tune measurements and resonance structure.

Both the experiment and simulation show the predicted diamond shape tune measurements from Figure 1. The simple hard edge model does a good job of giving an initial and quick prediction for the ring tunes.

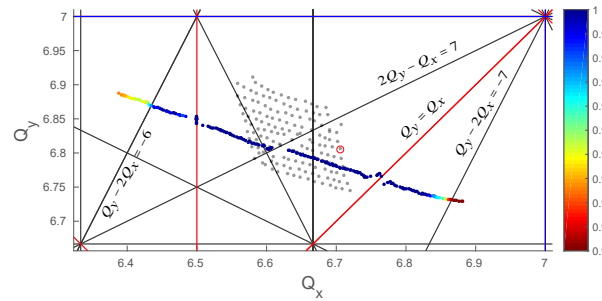


Figure 4: Long horizontal tune scan. Gray points are the same tune measurements from Figure 3. Color represents normalized beam survival.

Next a horizontal scan is done with the same 0.6 mA beam across a range of  $\Delta Q_x \approx 0.5$  as shown in Figure 4. The presence of several resonances up to third order is observed. A weak third order resonance at  $Q_y - 2Q_x = -6$  and a strong one at  $2Q_y - Q_x = 7$ . Both second order resonances,  $Q_x = 6.5$  and  $Q_x = Q_y$  are noticeable in the scan. The beginning of the integer stopbands at  $Q_x, Q_y = 7$  can be seen as beam is lost.

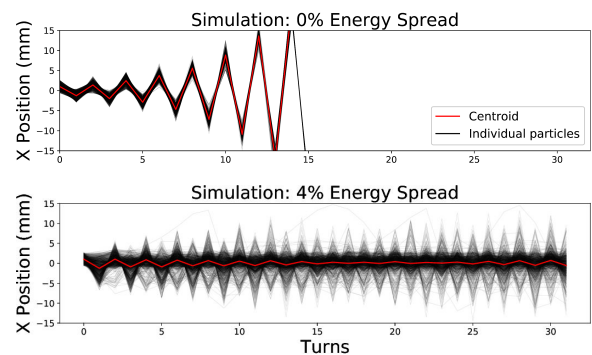


Figure 5: Simulated BPM data at the  $Q_x = 6.5$  resonance location. Simulation setup is the same as Figure 3.

Other than the integer stopbands, none of the other resonances cause measurable beam loss. This makes sense for weak third order resonances and a stable difference resonance, but not for the half integer stopband which should cause beam loss even in the presence of little space charge. While the exact phenomenon causing the resonance suppression is not yet understood, an early hypothesis suggests the

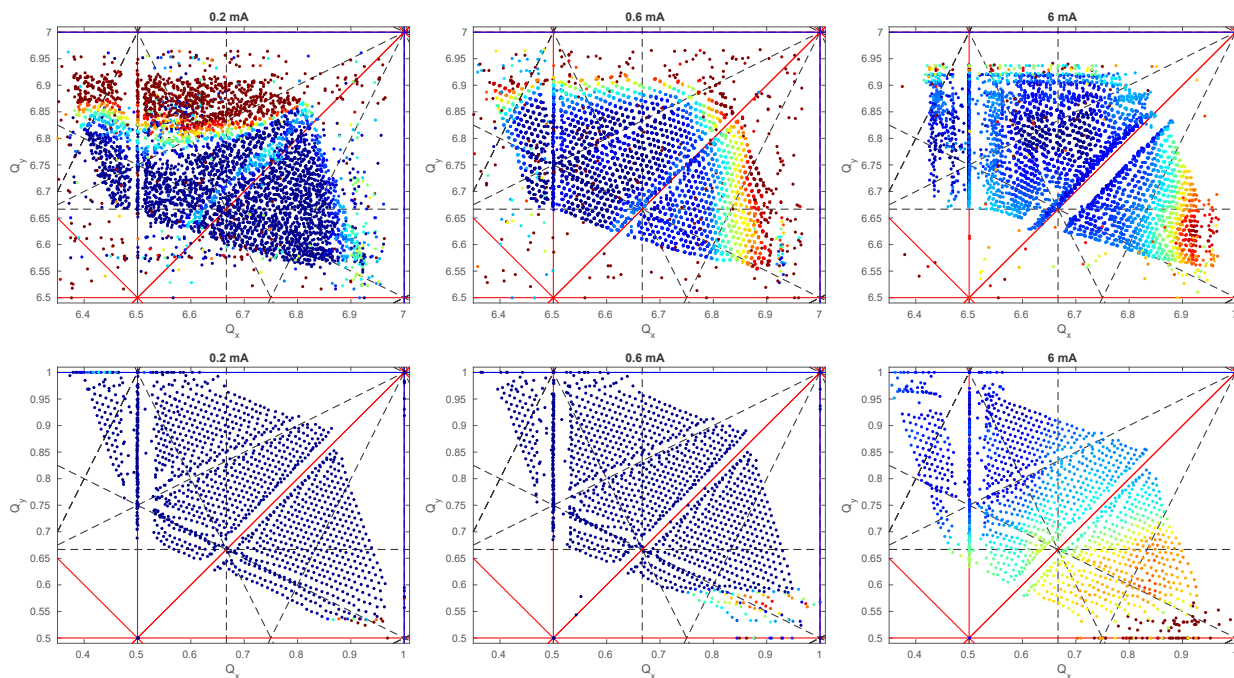


Figure 6: Large experimental grid scan for the 0.2 mA, 0.6 mA, and 6 mA beams at 10 keV. The top row is experimental measurement and the bottom row is simulation with WARP. Color represents normalized beam survival over the same range as Figure 4.

cause to be a large longitudinal energy spread from complex space charge related instabilities [9]; this energy spread causes a detuning of the resonance. Initial simulations in Figure 5 verify the behavior. Work on this topic is still in progress.

Lastly, a large grid scan is done over a quarter integer of tune space in Figure 6. A 0.2 mA, 0.6 mA, and 6 mA set of beams were used for the scans; these can be categorized as low space charge, space charge, and extreme space charge beams. Tune depressions listed in Table 1.

Table 1: Calculated Tune Depression for the Different Beams Used in the Gridded Scan Experiments

Beam (mA)	Tune Depression ( $Q/Q_0$ )
0.2	0.93
0.6	0.86
6	0.63

The low current (0.2 mA) beam had a large noise to signal ratio making it difficult to get accurate BPM measurements compared to the other two beams. Nonetheless, the other two beams give very detailed information about the nearby resonance structure. As the amount of space charge increases a few observations are made. The beginning of the  $Q_x = 7$  integer stopband is shifted further to the right, the  $Q_y = Q_x$  difference resonance bandwidth grows in size, and the third order resonance  $2Q_y - Q_x = 7$  seems to damp out. It is hard to say from the plots if the half integer  $Q_x = 6.5$  stopband is shifted or growing in size with increasing space charge. To

better understand these observations a set of more detailed scans, around the regions of interest, are planned.

The simulated grid scans accurately predict the same resonances measured experimentally. However, there is no measured resonance shift as seen in the experimental  $Q_x = Q_y$  difference resonance. Work is underway to better understand and incorporate magnet misalignments and field errors into the model to get better agreement for resonance bandwidths, shifts, and particle loss.

## CONCLUSION

Based on a FODO hard edge model, an experimental grid scan is developed. The grid scan is used to map a large portion of tune space to nearby resonance structure. This measurement is then done on different beams with varying amounts of space charge. Resonance structure dynamics as a function of space charge is observed. Measurements are also done through simulations to compare against experimental data.

A new set of more detailed scans are planned to better understand some of the initial resonance observations.

## ACKNOWLEDGEMENTS

This work was supported by the DOE-HEP (DE-SC0010301). Travel to NAPAC 2019 was supported by the APS Division of Beam Physics. Thanks to the UMER group for their helpful discussions.

## REFERENCES

- [1] M. Reiser, *Theory and design of charged particle beams*. Weinheim: Wiley-VCH, 2008.
- [2] R. Baartman, "Betatron resonances with space charge," *AIP Conf. Proc.*, vol. 448, no. 1, p. 56, 1998. doi:10.1063/1.56781
- [3] I. Hofmann, G. Franchetti, O. Boine-Frankenheim, J. Qiang, and R. D. Ryne, "Space charge resonances in two and three dimensional anisotropic beams," *Phys. Rev. ST Accel. Beams*, vol. 6, p. 024202, 2003. doi:10.1103/PhysRevSTAB.6.024202
- [4] M. Venturini and R. Gluckstern, "Resonance analysis for a space charge dominated beam in a circular lattice," *Phys. Rev. ST Accel. Beams*, vol. 3, p. 034203, 2000. doi:10.1103/PhysRevSTAB.3.034203
- [5] K. Kojima, H. Okamoto, and Y. Tokashiki, "Empirical condition of betatron resonances with space charge," *Phys. Rev. Accel. Beams*, vol. 22, p. 074201, 2019. doi:10.1103/PhysRevAccelBeams.22.074201
- [6] S. Bernal *et al.*, "RMS envelope matching of electron beams from "zero" current to extreme space charge in a fixed lattice of short magnets," *Phys. Rev. ST Accel. Beams* vol. 9, p. 064202, 2006. doi:10.1103/PhysRevSTAB.9.064202
- [7] J. Laskar, "Frequency analysis for multi-dimensional systems. Global dynamics and diffusion," *PhysicaD*, vol. 67, pp. 257–281, 1993. doi:10.1016/0167-2789(93)90210-R
- [8] A. Friedman *et al.*, "Computational Methods in the Warp Code Framework for Kinetic Simulations of Particle Beams and Plasmas," *IEEE Trans. Plasma Sci.* vol. 42, p. 01321, 2014. doi:10.1109/TPS.2014.2308546
- [9] B. L. Beaudoin *et al.*, "Multi-stream instability of a single long electron bunch in a storage ring," *Physics of Plasmas*, vol. 26, p. 052106, 2019. doi:10.1063/1.5095581